

INJECTION PAINTING IMPROVEMENTS IN THE J-PARC RCS

S. Kato[†], H. Harada, K. Horino, H. Hotchi, M. Kinsho, K. Okabe, P. K. Saha, Y. Shobuda, T. Takayanagi, N. Tobita, and T. Ueno
 J-PARC center, Japan Atomic Energy Agency, Ibaraki, Japan

Abstract

In the J-PARC 3GeV RCS, the injection painting is essential method for the reduction of the space charge force. In the transverse painting, the H⁻ beam from Linac is distributed on the large phase-space area of the ring orbit during multiple turns. To implement this method, painting magnets form the time variable beam orbit. Therefore, the precise output current control of the magnet power supply was required. Because the power supply was controlled by mainly feedforward signal, we developed the iterative tuning method for the optimum feedforward parameter determination. As a result, we could reduce the tracking error of the current compared to before. In addition, we improved the measurement method of the footprint of the painting process. In the adjustment of the painting, we adopted the additional correction of the current tracking based on the measured footprint. As a result, the intended painting process and area were achieved accurately. Thus we established the precise control technique of the injection painting.

INTRODUCTION

The 3 GeV rapid cycling synchrotron (RCS) of the Japan Proton Accelerator Research Complex (J-PARC) serves as a high intensity proton driver aiming to achieve a 1 MW beam power. The 400 MeV H⁻ beam from Linac is converted to proton at the injection point by the charge-exchange foil and stored during injection period of 0.5 ms repeatedly using the multi-turn charge-exchange injection method. The RCS accelerates protons up to 3 GeV with a repetition rate of 25 Hz. The beam is provided as the neutron source for the Materials & Life Science Experimental Facility (MLF) and as the injection beam for the 50 GeV main ring (MR). The current progress of the hardware and commissioning is described in the reference [1] in detail.

The RCS is adopted the transverse injection painting in order to distribute the injection beam on the large phase-space area intentionally and mitigate the space-charge force which can become the beam loss source. The scheme of that is as follows [2]. The schematic view of the injection area and the variation of the horizontal orbit during the painting are shown in Fig. 1. In the horizontal plane, during the 0.5 ms injection period, four shift-bump magnets (SB1-4) shape the fixed bump orbit. In addition, four paint-bump magnets (PB1-4) shape the time dependent bump orbit. Fig. 1a(A) shows the bump orbit at the injection start timing ($t = 0$). The injection track is matched to this bump orbit at the injection point. During multi-turn injection, the track of H⁻ beam is fixed and the

ring orbit is shifted slightly from the charge-exchange foil by decreasing the time dependent bump orbit height as shown in Fig. 1b(A) and Fig. 1c(A). Therefore, the injection beam changes its position and angle with respect to time along major axis in the phase-space ellipse of the ring orbit as shown in Fig. 1(B). As a result, the circulating beam becomes so broader compared with the Linac beam and the space-charge force is mitigated. In addition, the number of the charge-exchange foil hits by the circulating beams is decreased because the circulating beam is shifted from the foil.

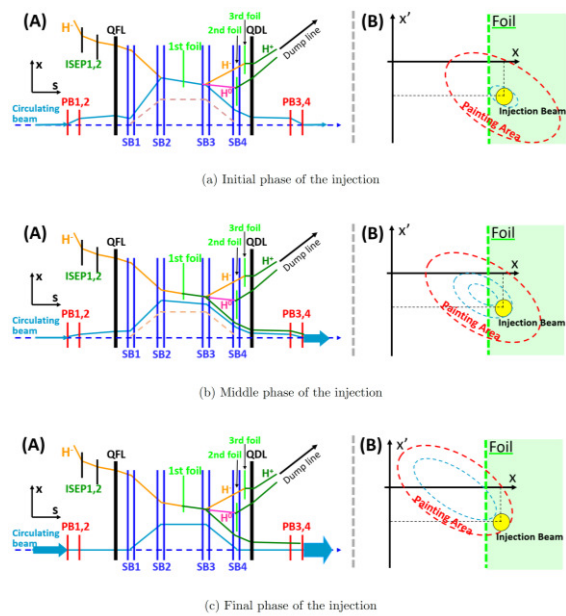


Figure 1: The horizontal orbit variation around the injection point during the injection period. Figure (A) indicates the orbits of the injection and the circulating beam. Figure (B) indicates the phase-space of the position and angle at the injection point.

In the vertical plane, two vertical paint magnets installed at the injection line change the injection beam angle at the injection point. The injection beam is brought closer to the central orbit from the edge of the painting area or vice versa in the phase-space ellipse of the ring orbit along angular axis. In the RCS, painting from the center to the outside in both horizontal and vertical phase-space is called Correlated Painting. On the other hand, painting from the outside to the center in vertical phase-space different from the horizontal painting is called Anti-Correlated Painting. When the injection beam position and angle are changed along the radial direction in proportion to the square root of the time, the beam is uniformly distributed on the phase-space area. Therefore, for

[†] skato@post.j-parc.jp

an elapsed injection time t , the horizontal time function is described by x and $x' \propto \sqrt{t/500 \mu\text{s}}$.

For the precise beam tuning and the beam loss control, it is required that the injection beam is painted correctly in the expected phase-space area. The accuracy of the injection painting depends on the precision of the output current adjustment of the magnet power supplies because the time variation of the orbit is generated by the PBs whose power supply are separated. Hence, the improvement of the current adjustment is essential. In addition, the closed orbit distortion (COD) caused by the unbalance of the PBs output during the injection period occurred up to ± 5 mm in the horizontal plane. Therefore, the improvement of the PBs output balance and the reduction of the COD should be also achieved by the precise current adjustment. To achieve the precise injection painting, the measurement technique for the time variable orbit height and the footprint of the painting process should be also developed to confirm the painted phase-space area. In terms of the efficiency of the beam tuning, the required time of the adjustment scheme including the current adjustment and the painting process observation should be short as much as possible.

In the RCS, the series of the injection painting adjustment has been improved to achieve these requirements and precise injection painting. In this paper, we present recent improvements focusing on the horizontal painting.

PRECISE CURRENT ADJUSTMENT OF THE POWER SUPPLY

Construction of the PB Magnet Power Supply

The basic construction of the PB magnet power supply is the four quadrant chopper circuit using IGBT switch. Actually, the power supply is operated as the two quadrant chopper circuit by cutting off two IGBT to avoid the reverse current flow in the magnet. As the chopper assemblies in front and back of the load, 18 sets of switch assembly are connected in parallel respectively. The switching frequency of IGBT is 50 kHz and the combined switching frequency is 600 kHz because 3 sets of switch share same switching pulse. The detail is described in the reference [3]. The rated maximum output current and the voltage is 29 kA and ± 1.2 kV, respectively.

For this power supply, the appropriate IGBT control signal should be generated in order to output intended current. The IGBT control signal is generated by mixing the analog feedback and feedforward signals in the control unit. To generate these two signals, we input the Set Current Waveform (SCW) and the Set Voltage Waveform (SVW). These two waveforms, the output current and the output current deviation from the SCW corresponding to the tracking error are shown in Fig. 2. The SCW is the target time variation pattern. The time decay waveform of the SCW follows the function $\sqrt{1 - (t/500 \mu\text{s})}$ from $t = 0$ though the function is proportional between $t = 0$ and $t = 88 \mu\text{s}$ to suppress the rate of change of the current within permissive voltage level. The control unit compares the

SCW and the output current and generates the analog feedback signal to reduce the tracking error. For this feedback, the significant current deviation is prevented even if the SCW is changed immediately and the power supply is protected. However, the tracking error cannot be obliterated completely when the output current changes largely during short time such as $500 \mu\text{s}$ because the response time constant of the feedback is approximately $20 \mu\text{s}$. Therefore, the SVW is also input as the analog feedforward signal. The value of the feedforward signal corresponds to the opening and closing times of the IGBT directly. Namely, the SVW corresponds to the target output voltage pattern. The value of the SVW is approximately scaled to the actual output voltage.

For the adjustment of the output current, we optimize the SVW. First, the initial SVW is calculated by the SCW (i), the inductance (L_m) and the resistance (R_m) of entire load circuit following the basic function $V = L_m(di/dt) + iR_m$. After that, we obtain the output current and modify the SVW repeatedly to minimize the tracking error.

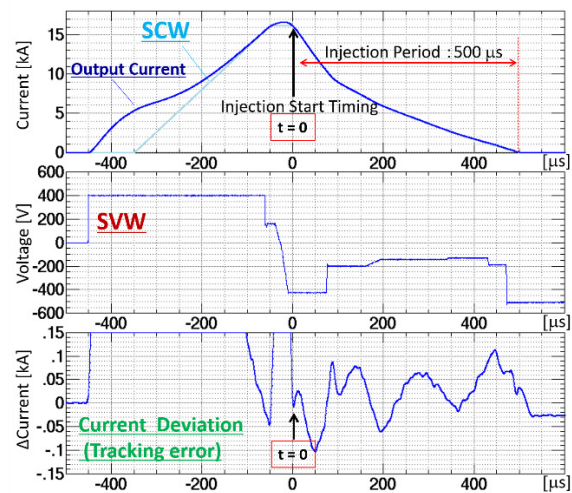


Figure 2: The typical waveforms of the SCW and output current (top), the SVW (center) and the current deviation (bottom) in the case of the PB1.

Improvement of the Adjustment Process

Previously, the accurate response of the output current to the change of the SVW was not comprehended. Therefore, each power supply had the tracking error which was more than ± 100 A even after adjustment. By the accumulation of the tracking errors of four power supplies, the COD was up to ± 5 mm because the error of 100 A generated the COD of 1 mm. In addition, the adjustment time was too long such as 1 hour per one power supply. Therefore, we comprehended the response and established the high accuracy automatic adjustment technique [4].

First, the response of the output current to the change of the SVW was measured. The measurement method is shown in Fig. 3. We prepared the trapezoidal waveforms of SCW shown in Fig. 3(a) and adjusted the SVW and the output current. The tracking error was ± 100 A or less. These adjusted waveforms were used as the reference waveforms. For the response measurement, the SVW

variation of the ΔV was added during ΔT_V shown in Fig. 3(b). Then, the current deviation from the reference waveform was measured. This was defined using two parameters of ΔI and ΔT_I as shown in Fig. 3(c). The ΔI and ΔT_I are the peak value of the current deviation and the required time, respectively. This measurement was performed for each magnet because the shapes of the magnet yoke and the internal constitutions of the power supply were different slightly. In the following, the results of the PB1 is shown on behalf of the other. For the relation between ΔT_I and ΔT_V , it was confirmed that the ΔT_I is larger than ΔT_V . The difference is larger than the dead time of the reaction to ΔV which is $10 \mu s$ because the feedback effect is gradual. For the relation between ΔI and ΔV for the several ΔT_V , the results are shown in Fig. 4(a). As shown, the ΔI is proportional to ΔV when the ΔT_V is fixed. The relation of $\Delta I/\Delta V$ and ΔT_V is shown in Fig. 4(b). The $\Delta I/\Delta V$ corresponds to the factor of proportionality. As shown, the rate of increase of the $\Delta I/\Delta V$ is less than that of the ΔT_V because the feedback effect suppresses the ΔI in the long ΔT_V condition. Although the relation of the $\Delta I/\Delta V$ and ΔT_V were not proportional, it became possible to obtain the $\Delta I/\Delta V$ for any ΔT_V conditions using the approximated quadratic function shown in Fig. 4(b).

These responses were also measured using some trapezoidal waveforms whose flat top current were different and the decay type waveforms as shown in Fig. 2. As a result, it was confirmed that these responses were same regardless of the current and the shape of the waveform.

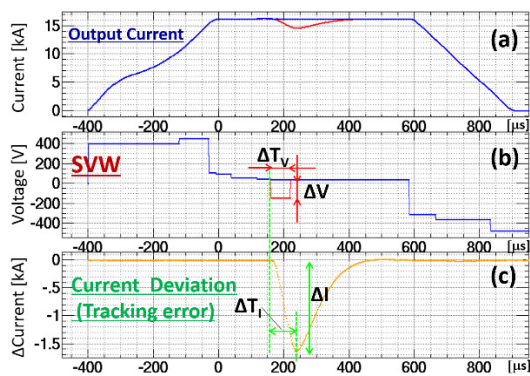


Figure 3: The reference waveform and the parameter definitions for the measurement of the output current response. The blue lines show the reference wave forms. The red lines show the modified wave forms. (a), (b), (c) show the output current, set voltage and current difference, respectively.

Second, the L_m and the R_m of the entire load circuit were measured in order to obtain the initial SVW which close to the final one. We prepared the trapezoidal waveforms of the SCW in the range of 4 to 16 kA and measured some relations between the SVW values as the voltage and the di/dt of the current deviation. After that, the L_m and R_m were calculated using the simultaneous equations. In other words, the L_m and R_m related to the SVW rather than real output voltage were measured.

Third, the new waveform of the SCW which had smooth curve at the both side of the flat top was adopted in order to minimize the tracking error before $t = 0$.

Finally, we developed the high accuracy adjustment tool using measured responses. For the first step, the di/dt of the current deviation was obtained with minimum time step of $2 \mu s$. After that, the ΔV which suppresses the di/dt was calculated using the results of the response measurement and applied to the SVW. These processes were repeated automatically.

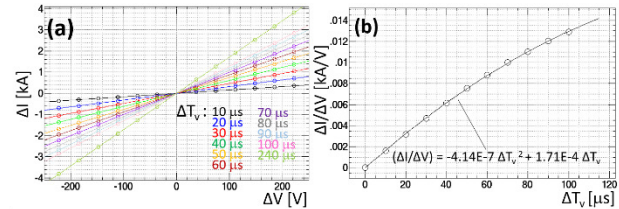


Figure 4: The relations between ΔI and ΔV for the several ΔT_V .

The adjustment results of the tracking error are shown in Fig. 5. The SVW calculated using new L_m and R_m was adopted as initial one. The number of adjustment iteration was 12. In Fig. 5, the previous adjustment results are also shown for comparison. As shown, the tracking error of the current could be reduced from the rising region of the SCW because of the new SCW and the iterative adjustment. As a result, the tracking error could be suppressed under ± 50 A. Because this remained value corresponded to the value of fluctuation of each output pulse, the high accuracy adjustment was achieved. Moreover, the adjustment time was reduced to be under 20 minutes per one power supply for the automatic tool.

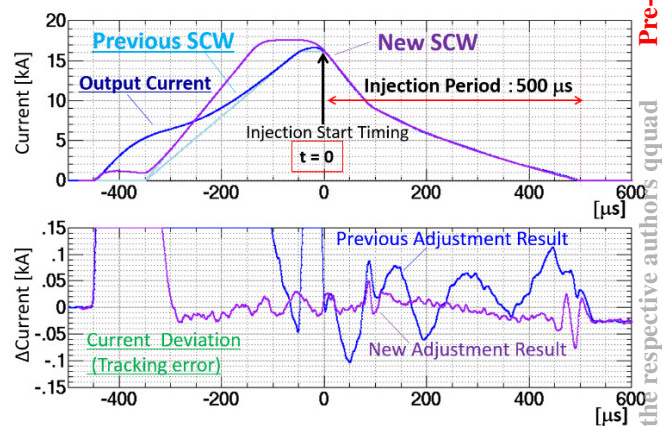


Figure 5: The results of the current adjustment. The blue lines show the previous pattern and the adjustment result. The purple lines show the developed pattern and the adjustment result.

MEASUREMENT METHOD OF THE PAINTING AREA

For the precise adjustment of the injection painting, it is required that the footprint of the painting process on the phase-space is measured continuously. For the horizontal

painting, the footprint and the final painted area can be obtained by measuring the time variation of the bump orbit height at injection point. Therefore, the measurement method which combines the online simulation model calculation and the COD measurement was established.

First, the COD was measured during injection period continuously. The multi-turn injection time was 100 μs . In order to obtain the COD from $t = 0$, the injection was completed until $t = 0$ by shifting just before the injection start timing specially. We obtained the COD by analyzing the signal of each BPM which had 4 electrodes [5]. The fourier transform (FT) was applied to the waveform of each electrode with time width of 51.2 μs . For the obtained spectrums, the peak value around the integer times of the revolution frequency of 614.25 kHz was regarded as the amplitude of the picked up signal. From the balance of these amplitudes of 4 electrodes, the orbit position at each BPM was determined. By repeating this manipulation from $t = 0$ with time step of 1 μs , we could obtain the time variable COD during injection period. As described above, the measurement of the COD during injection period required only 1 shot and shot time. The measurement was performed with and without the bump orbit of PBs and the COD caused by only PBs was extracted by subtracting these results.

Second, the kick angles of PBs expressed by K0 were estimated using the online simulation model fitting for the obtained COD. In the RCS, the model was constructed using SAD code. Its accuracy was confirmed by comparison with the measurement results of the various optical parameters in the beam commissioning up to now. For the fitting, only four K0 values of PBs were set as free parameter. Although the fitting target was the COD caused by only PBs, the fixed bump orbit formed by SBs was included in the fitting because this bump orbit closed between two BPMs located before and after of the injection point and did not relate that COD. The results are shown in Fig. 6. As a result, not only each K0 value but also the time variation of the bump orbit height at the injection point could be obtained continuously. Thus the footprint of the painting process could be measured.

PRECISE PAINTING ADJUSTMENT

Adjustment Process

For the precise painting adjustment, the methods of the current adjustment of the power supply and the measurement of the painting process were developed as described above section. In the RCS, the precise painting adjustment was established using these methods as follows.

First, the position and angle of the initial bump orbit at injection point was determined using the online simulation model and the measured beam parameter. The initial bump orbit is same with the fixed injection beam orbit. Therefore, the injection beam coordinate on the phase-space was determined to match the arbitrary painting area size at the end of injection period. Second, the initial K0 values of the four PBs which form the initial bump orbit was estimated by model fitting. And those values were

converted to the output current of the PB. The conversion factor was measured using the trapezoidal waveform of the PB whose output current was fixed during injection period. Specifically, the COD and K0 measurement was performed for the trapezoidal waveform. After that, the factor was derived from the analyzed K0 and the value of the output current monitor. It was confirmed that the relation between the K0 and the value of the current monitor was proportional by the various current measurements. Third, the output current of the PB power supply was adjusted. The SCW of decay waveform was constructed based on the obtained initial current value. And the tacking error was reduced by the automatic adjustment technique. Finally, the footprint of the painting process and the painting area were measured to confirm whether the painted area size and the footprint was correct or not.

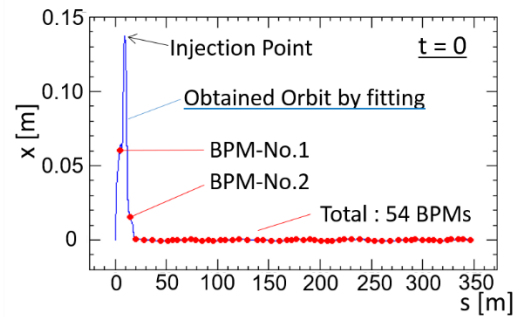


Figure 6: The obtained horizontal ring orbit by the COD fitting at $t = 0$. The red points are COD values measured by BPSs.

Results and Discussion

The result of the measured footprint of the painting process after adjustment is shown in Fig. 7 with red line. The target painting area was $150 \pi \text{ mm mrad}$. The line from center indicates the footprint of the painting process on the phase-space. As shown, the moving distance of the injection beam was insufficient. This result is equivalent to that the bump orbit height at $t = 0$ was insufficient. In other word, the output of the magnetic field was insufficient. The shortage was several hundred A at $t = 0$ for the decay waveform. This value was too large compared with the accuracy of the current adjustment. On the other hand, the bump height formed by the trapezoidal waveform whose current monitor value was same with that of decay waveform at $t = 0$ was sufficient. Therefore, this shortage of the magnetic field was caused by the existence of the decay region rather than the error of the conversion factor between K0 and the current.

By the investigation, it was found that the reason for this problem was the time delay of the current monitor value of the power supply in the decay region. For the PB power supply, the current monitor consisted of several Current Transformers (CT). Because the several CT were connected in parallel and these signals were synthesized, the generated current delayed in the synthesis circuit when the current changed quickly. In the decay region, the monitor value became bigger than the real output

current due to the time delay. Therefore, we were deceived into accepting the current as big. As a result, we set the current to be smaller.

Of course, the time delay of the magnetic field caused by the eddy current could be considered as the reason for the difference between the case of the trapezoidal and the decay waveform. However, the output of the magnetic field become bigger than the target value in the decay region in this case. Therefore, the magnetic field delay was not main reason though this effect was also contained.

In order to correct this issue, we regenerated the new SCW considering the shortage of the magnetic field and readjusted the output current. The shortage was converted to the current value and added to the original SCW. Some excessive current was also added. This correction was performed for the PB1 and PB2 which had larger output. Because the correction was based on the measured K0 value, it could potentially consider both time delay effects of the current monitor and the magnetic field.

The readjustment result is shown in Fig. 7 with blue line. The moving distance of the injection beam was enough improved by only one correction. In addition, the footprint followed the radial direction on the phase-space more accurate compared with before correction case because of the improvement of the output balance between PB1 and PB2.

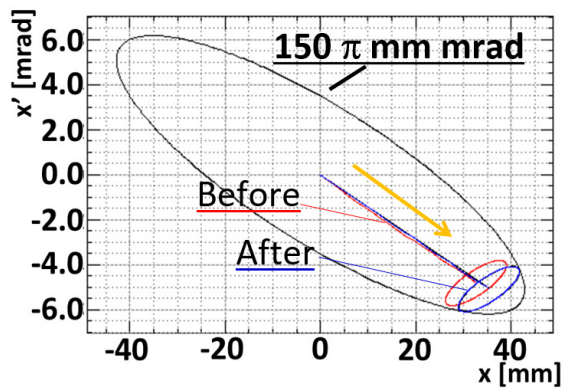


Figure 7: The measurement results of the footprint of the painting process on the horizontal phase-space of the ring orbit. The black ellipse indicates the target painting area. The orange arrow indicates the painting direction. The red and blue lines indicate the footprint of the painting process before and after readjustment, respectively. The red and blue ellipses indicate the injection beam of 4π mm mrad.

The COD caused by the unbalance of the PB output during injection period is shown in Fig. 8. The amplitude of that could be reduce compared with previous one by the developed current adjustment technique and the correction. The amplitude became under ± 2 mm during injection period. From these results, the precise painting adjustment method including the correction based on the measured K0 was established and the precise injection painting was achieved.

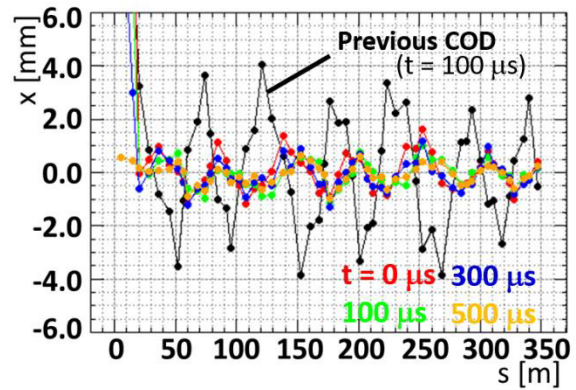


Figure 8: The CODs measured after painting adjustment. The black line is the previous result. The other lines indicate that of each time shown in the figure.

SUMMARY

In the RCS, the control of the injection painting was improved. To reduce the tracking error of the output current of the PB which directly relates the painting accuracy, the response of the output current to the feedforward signal which was control knob was examined. In addition, the automatic adjustment technique was developed using this result in order to reduce the current adjustment time of the PB power supply which occupies a lot of the beam turning session could be reduce. As a result, the required time and the accuracy became 1/3 and 2 times compared with previous one, respectively. To obtain the footprint of the painting process on the phase-space and the painted area size, the measurement method which combined the model calculation and the COD measurement was also established. The paining adjustment was performed using these developed methods. During the adjustment, it was found that the gap between the monitor current value of PB power supply and the outputted kick angle occurred. Therefore, the correction based on the measured kick angle was adopted to solve this issue. Finally, it became possible to distribute the injection beam on the target paint area correctly because of these improvements. In addition, the COD caused by the unbalance of the PB current also reduced. Therefore, we established the precise control of the injection painting.

REFERENCES

- [1] H. Hotchi et al., "THE PATH TO 1 MW -BEAM LOSS CONTROL IN THE J-PARC 3-GeV RCS-", in this conference.
- [2] H. Harada, KEK Report No. 2009-7.
- [3] T. Takayanagi et al., "Development of a large-current high-precision pulse power supply", *Electrical Engineering in Japan*, vol. 166, Issue 3, 2009, pp.62-72.
- [4] S. Kato et al., in *Proc. of the 12th Annual Meeting of Particle Accelerator Society of Japan*, Tsuruga, Japan, 2015, pp.1180-1184.
- [5] N. Hayashi et al., in *Proc. Of the EPAC08*, Genoa, Italy, 2008, pp. 1128-1130.